A bifunctional cloak using transformation media

J. Y. Li,[1] Y. Gao,[1,2] and J. P. Huang[1,a)]
[1]*Department of Physics, State Key Laboratory of Surface Physics, and Key Laboratory of Micro and Nano Photonic Structures (Ministry of Education), Fudan University, Shanghai 200433, China*
[2]*Department of Applied Physics, School of Science, Shanghai Second Polytechnic University, Shanghai 201209, China*

(Received 26 December 2009; accepted 18 August 2010; published online 5 October 2010)

We theoretically explore a type of bifunctional cloak possessing both electrical and thermal cloaking functionality. We employ a composite material to design the cloak shell. By using effective medium theory, the effective electrical and thermal conductivities of the composite material should meet the perfect conductivity profile calculated from the coordinate transformation approach. In the design, we choose nonspherical nanoparticles with appropriate electrical and thermal conductivities, shape aspects, and volume fractions. Furthermore, finite element simulations are performed to verify the properties of such bifunctional cloaks. © *2010 American Institute of Physics*.
[doi:10.1063/1.3490226]

I. INTRODUCTION

In the past few years, researchers have shown great interest in the application of making something invisible. In 2006, Pendry *et al.*[1] proposed an interesting idea, using the transformation optics approach to design an invisibility cloak. Independently, an optical conformal mapping method has been used to design a refractive index profile that guides light rays around an object in the geometric optics limit.[2] And there are also other routes to achieve invisibility, such as scattering-cancellation properties of plasmonic materials with low positive or negative permittivity,[3–6] and anomalous localized resonance.[7] Based on metamaterials,[8,9] the first experimental design of an invisibility cloak was realized at microwave frequencies.[10] Researchers then designed invisibility cloaks working at optical frequencies,[11] and we designed a multifrequency cloak with a multishell using transformation media.[12] The coordinate transformation approach has been extended to other fields including acoustics,[13] conduction,[14,15] elastic wave,[16] and matter waves.[17] The fundamental reason for such an extension is that the governing equations describing these systems are form invariant under coordinate transformations,[18] just as Maxwell's equations are form invariant in the original and transformed spaces.

The cloaking of electrical conduction can be traced back to the pioneering work of Greenleaf *et al.* in 2003.[19] However, almost all previous research about invisibility cloaks focused on a single cloaking function. Yet, an ideal cloaking device should possess masking functionality in multiple regimes. In this work, we explore a type of bifunctional cloak possessing both electrical and thermal cloaking functionality. We design the bifunctional cloak using transformation media with a composite material for the cloak shell. By using effective medium theory (EMT), the effective electrical and thermal conductivities of the composite material should fit the perfect anisotropic conductivity profile calculated from the coordinate transformation approach. In the design, we suitably adjust material parameters, such as electrical and thermal conductivities, shape aspect ratios, and volume fractions of nonspherical nanoparticles. As for the thermal conductivity, we also take into account the interfacial thermal resistance of the nanoparticles used in the composite material. Furthermore, by using the software COMSOL MULTIPHYSICS 3.5, finite element simulations are performed to confirm the bifunctionality of the cloak. This work provides an approach to investigate bifunctional cloaks.

II. COORDINATE TRANSFORMATION AND EMT

We first investigate the governing equations to describe the system, considering the electrical and thermal conductivities. Without the source term and the external current, the electrical conduction equation can be written as,

$$\nabla \cdot [\sigma \nabla V] = 0, \tag{1}$$

where V is the electrical potential and σ is the electrical conductivity. Similarly, if we consider a steady state of thermal conduction, without the temperature changing with time and additional heat sources, the governing equation of the heat flux has the same form as Eq. (1) (changing V to T and σ to κ). Here T represents temperature and κ is thermal conductivity. The conduction equations are form invariant under coordinate transformations.[18]

We investigate the spherical case, where a spherical region with radius R_2 is compressed into a concentric spherical shell $R_1 < R < R_2$ under the coordinate transformation in spherical coordinates (R, θ, φ),

$$R' = \frac{R_2 - R_1}{R_2} R + R_1, \quad \theta' = \theta, \quad \varphi' = \varphi. \tag{2}$$

Based on the form invariance of the conduction equations in the original and transformed spaces, we can obtain the electrical conductivity tensor of the transformation media,

a)Electronic mail: jphuang@fudan.edu.cn.

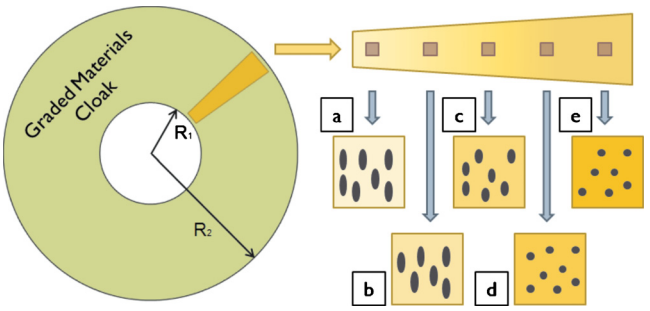

FIG. 1. (Color online) Schematic diagram of our designed cloak. R_1 and R_2 are the radii of the inner and outer boundaries of the cloaking shell, respectively. The nonspherical nanoparticles are distributed along the radius of the cloak with various shape aspects and volume fractions.

$$\sigma' = \frac{\mathbf{A}\sigma_0\mathbf{A}^T}{\det \mathbf{A}}, \tag{3}$$

where $\mathbf{A}$ is the Jacobian transformation matrix between the transformed and original coordinates, and σ_0 is the thermal conductivity in the original coordinates. Thereby, we can obtain the electrical conductivity tensor of the material in the cloaking shell in spherical coordinates (R, θ, φ),

$$\sigma_R = \frac{R_2}{R_2 - R_1}\left(\frac{R - R_1}{R}\right)^2 \sigma_0,$$

$$\sigma_\theta = \frac{R_2}{R_2 - R_1}\sigma_0,$$

$$\sigma_\varphi = \frac{R_2}{R_2 - R_1}\sigma_0. \tag{4}$$

By using the same method, we also achieve the thermal conductivity tensor of the material in the cloaking shell,

$$\kappa_R = \frac{R_2}{R_2 - R_1}\left(\frac{R - R_1}{R}\right)^2 \kappa_0,$$

$$\kappa_\theta = \frac{R_2}{R_2 - R_1}\kappa_0,$$

$$\kappa_\varphi = \frac{R_2}{R_2 - R_1}\kappa_0. \tag{5}$$

Here σ_0 in Eq. (4) and κ_0 in Eq. (5) are the electrical and thermal conductivities in the original coordinates, respectively, which are also used as the background parameters in our design. The conductivities in θ and φ directions are equal, and therefore Eqs. (4) and (5) can be written as two parts, namely, the radial conductivity σ_r or κ_r and the tangential conductivity σ_t or κ_t.

Our goal is to use a composite material to meet the perfect material parameters calculated by the coordinate transformation approach. In our design, we distribute nonspherical nanoparticles of electrical conductivity σ_m and thermal conductivity κ_m into a homogeneous medium with electrical conductivity σ_i and thermal conductivity κ_i, as shown schematically in Fig. 1. The effective electrical conductivity of the composite material is given by the Bruggeman "shape-dependent" EMT,[20–22]

$$\frac{\sigma_m - \sigma_{r,t}}{\sigma_{r,t} + \Gamma_{r,t}(\sigma_m - \sigma_{r,t})}p + \frac{\sigma_i - \sigma_{r,t}}{\sigma_{r,t} + \Gamma_{r,t}(\sigma_i - \sigma_{r,t})}(1-p) = 0, \tag{6}$$

where, p is the volume fraction of the nonspherical nanoparticles, and Γ_r and Γ_t are the geometrical shape factors along the radial and tangential directions, respectively.

For the corresponding thermal conductivity, we take into account the interfacial thermal resistance of the nanoparticles in the composite material. So we write the thermal conductivity of the nanoparticles coated with layers of thickness δ and conductivity κ_s as,[23]

$$\kappa_m' = \frac{\kappa_m}{1 + \frac{R_{\mathrm{Bd}}}{r_a}\kappa_m}, \tag{7}$$

$$R_{\mathrm{Bd}} = \lim_{\delta\to 0, \kappa_s \to 0}(\delta/\kappa_s), \tag{8}$$

where κ_m is the original thermal conductivity of the nonspherical nanoparticles, and r_a is the average radius of the nanoparticles. The value of R_{Bd} depends on the chosen materials.[23,24] The interfacial thermal resistance depends on the aspect ratio of the nanoparticles. However, if the aspect ratio is large, Eq. (7) can changes significantly,[23,24] which has been demonstrated in these two references and is valid as an approximation for calculation. From the results of the equations of the electrical part, we find that the aspect ratios are small, so we treat the nanaoparticles as spheres.

Considering the interfacial thermal resistance of the nonspherical nanoparticle, the effective thermal conductivity of the composite material can be calculated by EMT,

$$\frac{\kappa_m' - \kappa_{r,t}}{\kappa_{r,t} + \Gamma_{r,t}(\kappa_m' - \kappa_{r,t})}p + \frac{\kappa_i - \kappa_{r,t}}{\kappa_{r,t} + \Gamma_{r,t}(\kappa_i - \kappa_{r,t})}(1-p) = 0. \tag{9}$$

In order to get the same results for $\Gamma_{r,t}$ and p by solving Eqs. (4) and (6), or Eqs. (5) and (9), we should choose the parameters as $\sigma_m = n_1\sigma_0$, $\kappa_m' = n_1\kappa_0$, $\sigma_i = n_2\sigma_0$, and $\kappa_i = n_2\kappa_0$, where n_1 and n_2 are coefficients of proportionality. This means that the equivalent thermal conductivity κ_m' of the nonspherical nanoparticles considering the interfacial thermal resistance and the electrical conductivity σ_m of the nonspherical nanoparticles must satisfy the same ratio with respect to the thermal and electrical conductivities in the original coordinates. And the thermal and electrical conductivities of the host material used in the composite material should also satisfy the same ratio with respect to the thermal and electrical conductivities in the original coordinates. In the following calculations, we choose $\sigma_m = 30\sigma_0$ and $\sigma_i = 0$. We can determine the values of the geometrical shape factors by solving Eqs. (4) and (6) or Eqs. (5) and (9). The geometrical shape factor in the radial direction is always greater than 1/3 with the parameters chosen in this work, which means that the nonspherical nanoparticles used in the composite material exist in the form of oblate spheroids with three principle axes c

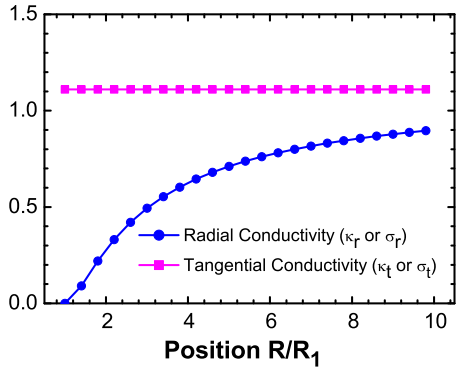

FIG. 2. (Color online) The normalized values of the effective electrical and thermal conductivities at different positions in the cloak shell, with $R_1:R_2=1:10$.

$<b=a$. On the other hand, geometrical shape factors Γ_r and Γ_t are functions of the shape aspect ratio $\gamma=a/c$,[25]

$$\Gamma_r(\gamma)=\frac{\gamma}{\gamma-1}-\frac{\gamma\sec^{-1}\sqrt{\gamma}}{(\gamma-1)^{3/2}},$$

$$\Gamma_t(\gamma)=\frac{1}{2}\left(\frac{\gamma\sec^{-1}\sqrt{\gamma}}{(\gamma-1)^{3/2}}-\frac{1}{\gamma-1}\right), \quad (10)$$

and the geometrical shape factors satisfy the relation $2\Gamma_t+\Gamma_r=1$. It is worth noting that $\gamma=1$ denotes the spherical case. We can now determine the shape aspect ratios of the nonspherical nanoparticles used in the composite material for configurating the cloaking shell.

III. RESULTS AND DISCUSSION

Figure 2 denotes the normalized values of the effective electrical and thermal conductivities at different positions in the cloak shell with $R_1:R_2=1:10$. As we can see, the electrical and thermal conductivities are anisotropic, and the radial electrical and thermal conductivities change as the position R/R_1 changes, while the tangential component of the electrical and thermal conductivities are almost the same as the position changes, simplifying real fabrication. In the design, the nonspherical nanoparticles are distributed along the radius of the cloak with different shape aspects and volume fractions.

To prove the proposed bifunctional cloak with both electrical and thermal cloaking effects, we use the software COMSOL MULTIPHYSICS 3.5 to perform finite element simulations of the design. Figure 3 displays the finite element simulation results of the cross section of our designed cloak with $R_1:R_2=1:3$. In the simulations, the boundary conditions are set to 300 K and 200 V at the top boundary, and 100 K and 0 V at the bottom boundary. Arrows in Fig. 3(a) display the path way of the current density in the cloaking shell, and the color surface represents the electric potential. Arrows in Fig. 3(b) denote the path way of heat flux in the cloaking shell; temperature distribution is indicated by color. We can see that the current and heat fluxes go smoothly around the inner domain and eventually returns to their original pathways. In this case, the object inside the inner domain is protected from the invasion of external current and heat fluxes. The simulation results clearly demonstrate the appearance of bifunctional cloaking effects with simultaneous electrical and thermal cloaking.

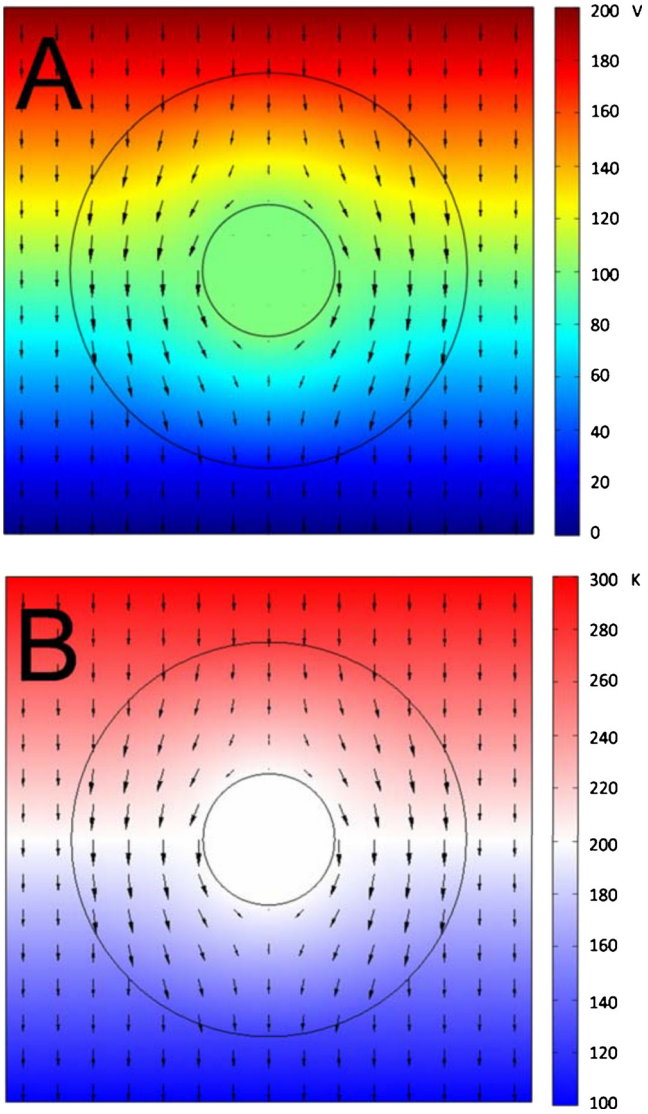

FIG. 3. (Color online) Finite element simulations of the cross section of our designed cloak with $R_1:R_2=1:3$. Parameters are set to be 300 K and 200 V at the top boundary and 100 K and 0 V at the bottom boundary. (a) The arrows display the pathway of the current density in the cloaking shell; color surface represents the electric potential. (b) Here arrows denote the pathway of heat flux in the cloaking shell and the temperature distribution is indicated by the color surface.

We now investigate further the geometric and material parameters of the cloaking shell to achieve invisibility. The particle aspect ratio decreases as the position R/R_1 increases, and the volume fraction of the nonspherical nanoparticles increases gradually as R/R_1 increases, as shown in Fig. 4(a). Figure 4(b) shows that the geometrical shape factor in the radial direction decreases as R/R_1 increases, while the geometrical shape factor in the tangential direction increases as R/R_1 increases. The geometrical shape factor in the radial direction is always larger than 1/3 with the parameters used in our work, which means that the nonspherical nanoparticles used in the composite material have the shape of an oblate spheroid. Figure 4(c) displays the normalized values of the effective electrical and thermal conductivities at different po-

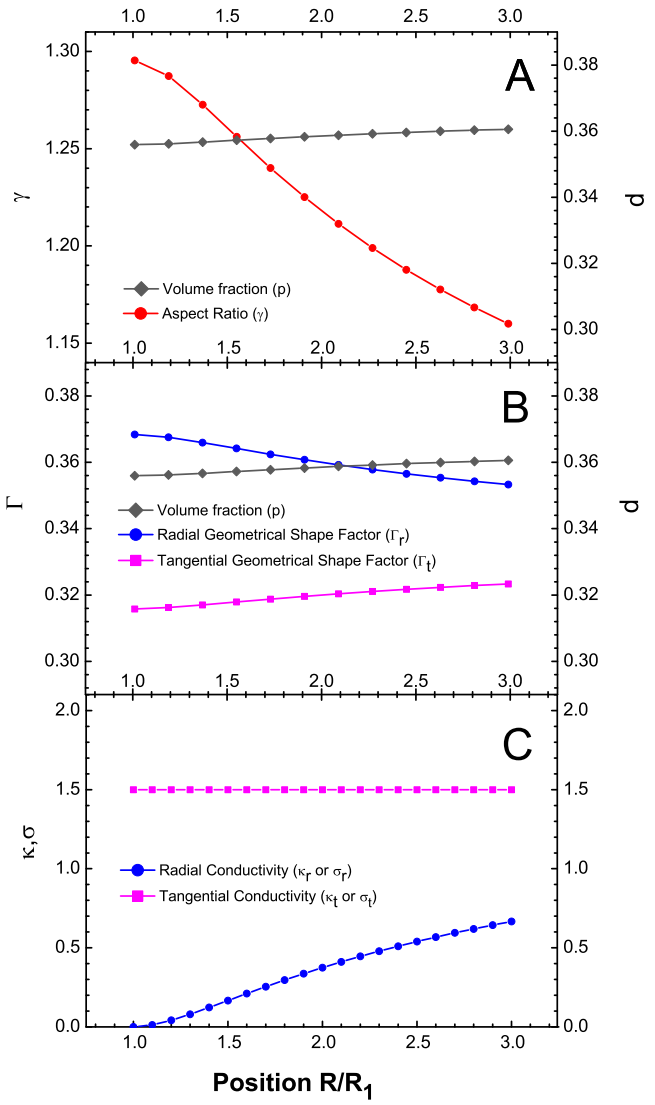

FIG. 4. (Color online) The calculation results for a cloak with $R_1:R_2=1:3$. (a) The shape aspect ratio and volume fraction of the nonspherical nanoparticles as functions of position (indicated by R/R_1). (b) The radial and tangential part of geometrical shape factors as functions of R/R_1. (c) The normalized values of the effective electrical and thermal conductivities at different positions in the cloak shell with $R_1:R_2=1:3$.

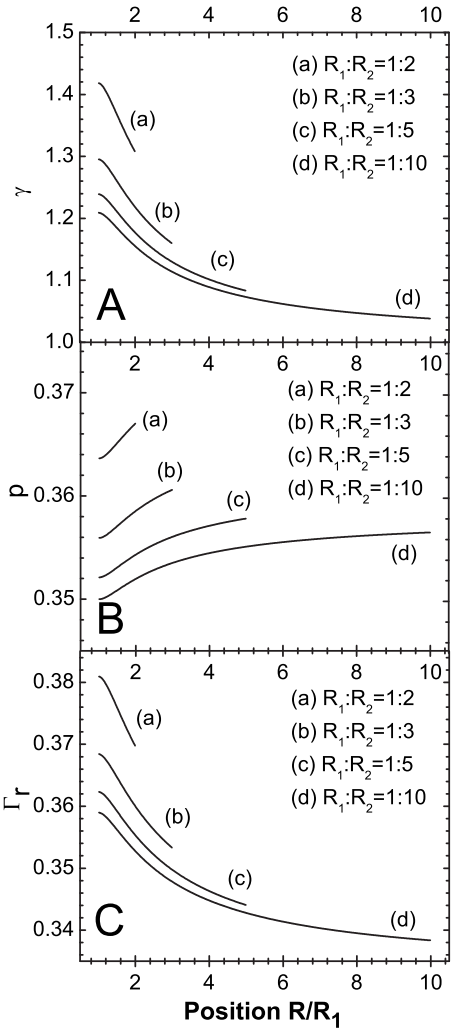

FIG. 5. Comparison of the parameters for different cloaks with $R_1:R_2=1:2$, 1:3, 1:5, and 1:10. (a) The shape aspect ratio γ of nonspherical nanoparticles, (b) the volume fraction p, and (c) the radial geometrical shape factor.

sitions in the cloak shell with $R_1:R_2=1:3$. We further compare the parameters for different bifunctional cloaks with $R_1:R_2=1:2$, 1:3, 1:5, and 1:10. Figure 5(a) is for the shape aspect ratio γ of nonspherical nanoparticles, Fig. 5(b) is for the volume fraction p, and Fig. 5(c) is for the radial geometrical shape factor.

IV. CONCLUSIONS

In summary, we propose a design of bifunctional cloak with both electrical and thermal cloaking functionality using transformation media. On the basis of EMT, we design the cloak shell to meet the perfect conductivity profile calculated by using the coordinate transformation approach. In the design, we choose nonspherical nanoparticles used in a composite material with appropriate electrical and thermal conductivities, shape aspects, and volume fractions. The equivalent thermal conductivity κ_m' of the nonspherical nanoparticles considering the interfacial thermal resistance and the electrical conductivity σ_m of the nonspherical nanoparticles must satisfy the same ratio with respect to the thermal and electrical conductivities in the original coordinates. Besides, the thermal and electrical conductivities of the host material used in a composite material should also satisfy the same ratio with respect to the thermal and electrical conductivities in the original coordinates. It is worth noting that, besides thermal conduction under our consideration, heat can also be transferred by thermal radiation and/or convection, and that often more than one process occurs in a particular situation. In fact, we can design various multifunctional cloaks by using a similar method.

ACKNOWLEDGMENTS

We acknowledge the financial support by the National Natural Science Foundation of China under Grant Nos. 10874025 and 11075035 and by Chinese National Key Basic Research Special Fund under Grant No. 2006CB921706. We also appreciate the support from Graduate Innovation Fund of Fudan University.

[1]J. B. Pendry, D. Schurig, and D. R. Smith, Science **312**, 1780 (2006).
[2]U. Leonhardt, Science **312**, 1777 (2006).
[3]A. Alù and N. Engheta, Phys. Rev. Lett. **100**, 113901 (2008).
[4]M. Kerker, J. Opt. Soc. Am. **65**, 376 (1975).
[5]A. Alù and N. Engheta, Phys. Rev. E **72**, 016623 (2005).
[6]L. Gao, T. H. Fung, K. W. Yu, and C. W. Qiu, Phys. Rev. E **78**, 046609 (2008).
[7]G. W. Milton and N.-A. Nicorovici, Proc. R. Soc. London, Ser. A **462**, 3027 (2006).
[8]R. A. Shelby, D. R. Smith, and S. Schultz, Science **292**, 77 (2001).
[9]J. Yao, Z. W. Liu, Y. M. Liu, Y. Wang, C. Sun, G. Bartal, A. Stacy, and X. Zhang, Science **321**, 930 (2008).
[10]D. Schurig, J. J. Mock, B. J. Justice, S. A. Cummer, J. B. Pendry, A. F. Starr, and D. R. Smith, Science **314**, 977 (2006).
[11]W. Cai, U. K. Chettiar, A. V. Kildishev, and V. M. Shalaev, Nat. Photonics **1**, 224 (2007).
[12]Y. Gao, J. P. Huang, and K. W. Yu, J. Appl. Phys. **105**, 124505 (2009).
[13]H. Y. Chen and C. T. Chan, Appl. Phys. Lett. **91**, 183518 (2007).
[14]T. Y. Chen, C. N. Weng, and J. S. Shen, Appl. Phys. Lett. **93**, 114103 (2008).
[15]C. Z. Fan, Y. Gao, and J. P. Huang, Appl. Phys. Lett. **92**, 251907 (2008).
[16]M. Farhat, S. Guenneau, and S. Enoch, Phys. Rev. Lett. **103**, 024301 (2009).
[17]S. Zhang, D. A. Genov, C. Sun, and X. Zhang, Phys. Rev. Lett. **100**, 123002 (2008).
[18]G. W. Milton, M. Briane, and J. R. Willis, New J. Phys. **8**, 248 (2006).
[19]A. Greenleaf, M. Lassas, and G. Uhlmann, Physiol. Meas **24**, 413 (2003).
[20]T. K. Xia, P. M. Hui, and D. Stroud, J. Appl. Phys. **67**, 2736 (1990).
[21]C. Y. You, S. C. Shin, and S. Y. Kim, Phys. Rev. B **55**, 5953 (1997).
[22]L. H. Shi and L. Gao, Phys. Rev. B **77**, 195121 (2008).
[23]C. W. Nan, R. Birringer, D. R. Charke, and H. Gleiter, J. Appl. Phys. **81**, 6692 (1997).
[24]L. Gao, X. F. Zhou, and Y. L. Ding, Chem. Phys. Lett. **434**, 297 (2007).
[25]T. G. Mackay and A. Lakhtakia, J. Opt. A, Pure Appl. Opt. **7**, 669 (2005).